Taylor & Francis
Taylor & Francis Group

Mathematical and Computer Modelling of Dynamical Systems

Methods, Tools and Applications in Engineering and Related Sciences

ISSN: 1387-3954 (Print) 1744-5051 (Online) Journal homepage: http://www.tandfonline.com/loi/nmcm20

Mathematical modelling of the oxygen uptake kinetics during whole-body endurance exercise and recovery

John F. Moxnes & Øyvind Sandbakk

To cite this article: John F. Moxnes & Øyvind Sandbakk (2018) Mathematical modelling of the oxygen uptake kinetics during whole-body endurance exercise and recovery, Mathematical and Computer Modelling of Dynamical Systems, 24:1, 76-86, DOI: 10.1080/13873954.2017.1348364

To link to this article: https://doi.org/10.1080/13873954.2017.1348364

MATHEMATICAL AND COMPUTER MODELLING OF DYNAMICAL SYSTEMS, 2018
VOL. 24, NO. 1, 76–86
https://doi.org/10.1080/13873954.2017.1348364

Taylor & Francis
Taylor & Francis Group

ARTICLE

Mathematical modelling of the oxygen uptake kinetics during whole-body endurance exercise and recovery

John F. Moxnes[a] and Øyvind Sandbakk[b]

[a]Land Systems Division, Norwegian Defence Research Establishment, Kjeller, Norway; [b]Center for Elite Sports Research, Department of Neuromedicine and Movement Science, Norwegian University of Science and Technology, Trondheim, Norway

ABSTRACT

In this study, we elucidate four different mathematical models of the kinetics of oxygen uptake during whole-body endurance exercise at different intensities and throughout the subsequent recovery periods. We employ the hypothetical inductive–deductive method and forecast four different models for the oxygen kinetic. The VO_2 development using these models compared with experimental results where an elite cross-country skier performed laboratory tests while running with poles on a treadmill, in which the rate of oxygen uptake and blood lactate concentration as a function of time were measured. The most developed model accounted for the delayed superimposed slow component of oxygen uptake and the influence of lactic power production on the oxygen kinetics. The rate of change in oxygen with this model is consistent with the accumulated oxygen deficit model and matched the data well, even for intensities above the lactate threshold and during recovery.

ARTICLE HISTORY
Received 26 February 2016
Accepted 26 June 2017

KEYWORDS
VO_2 kinetics; aerobic power; anaerobic power; lactate concentration

Introduction

Cross-country skiing is a demanding endurance sport where the rate of work and metabolic intensity are changing continuously across the varying terrain [1,2]. In such sports, the oxygen uptake (VO_2) kinetics that describes the rate of change in VO_2 following the onset of exercise or a change in work rate is of significant importance.

The pulmonary oxygen uptake is used as a proxy for VO_2, and it rise in a nearly exponential fashion following the onset of exercise. This has been described by three distinct phases: Phase I is the first 15–25 s, named the cardio-dynamic phase representing the circulatory transit delay of VO_2 from muscles to lungs [3]; Phase II is the increase in VO_2 reflecting the adjustment of VO_2 in the active skeletal muscles; and Phase III is the steady-state phase of VO_2 during moderate-intensity exercise [4,5].

At high intensities above the lactate threshold (LT), a delayed slow component of VO_2 is normally initiated 100–200 s following commencement of exercise [6–9]. This slow component generates a steady-state situation of VO_2 that is either right below or equal to the maximal VO_2 (VO_2max). Although the mechanism underlying the slow component is not well understood, the amplitude and rate of change of the slow component are both correlated with changes in blood lactate concentration during heavy exercise [10]. In addition, a slow increase in VO_2 during prolonged submaximal intensity, referred to as VO_2 drift, is also observed at intensities well below the LT [11].

CONTACT John F. Moxnes john-f.moxnes@ffi.no

To model VO_2 kinetics in response to exercise, differential equations with a smooth function of time and intensity have been shown to provide more accurate estimations over a continuum of exercise intensities than the abovementioned three-phase model where the phases turn on and off at discrete time intervals [4]. In the current study, we outline four different models for describing the VO_2 kinetics during and after endurance exercise. Model 1 is Stirling et al.'s [4] differential equation. Model 2 is a first-order differential equation model where the time development of VO_2 at a given work rate is used as input [12,13]. Here, VO_2 kinetics is assessed using the difference between requirements of aerobic power and the available aerobic power to fully accommodate the work rate [14]. Model 3 is an extension of Model 2 where we additionally account for reduced chemical- and contraction-coupling efficiencies associated with production of lactic power. Thus, this model induces a superimposed delayed slow component of VO_2. Model 4 is a theoretically derived model that accounts for the superimposed slow component and that the production of lactic power may directly influence the aerobic kinetics.

The purpose of this study was to elucidate these four models for the kinetics of VO_2 during whole-body endurance exercise at different exercise intensities and the subsequent recovery periods. These models were fitted to the characteristics of an elite cross-country skier-performing laboratory tests while running with poles on a treadmill, in which the rate of VO_2 and blood lactate concentration were measured as a function of time.

In our model development, we have aimed to increase the level of sophistication by including different components and compare how they capture the main physiological behaviour. Specifically, Models 1 and 2 differ in the way they handle intensities above the maximal rate of oxygen uptake. Model 3 additionally handles the superimposed delay component, while Model 4 differs from the other three since the oxygen kinetic is dependent on the lactate kinetic.

Methods

Overall design

Initially, the four models described above where outlined. The mathematical computation programme Mathematica 9 (Wolfram Research Incorporation, Champaign, IL, USA) was used to simulate the kinetics of VO_2 during whole-body exercises and recovery. The outputs of the simulation models were compared with experimental data where the skier ran with poles on a treadmill at various exercise intensities. Here, the VO_2 and blood lactate concentration were measured as a function of time.

Model development

Intracellular production of ATP occurs either aerobically (in the mitochondria by oxidative phosphorylation) or anaerobically due to glycolysis/glycogenolysis (generating lactic anaerobic power) as well as breakdown of phosphocreatine (PCr) into creatine (Cr) (i.e. ADP + PCr gives ATP + Cr in the creatine kinase [CK] reaction). The symbol η represents contraction-coupling efficiency while η_a denotes the chemical-coupling efficiency during aerobic production of ATP. The symbol η_g represents chemical-coupling efficiencies during production of ATP through glycolysis/glycogenolysis (G), and η_{ck} denotes the chemical-coupling efficiencies during ATP production by CK reaction. The work power (i.e. the time derivate of the sum of external work and internal work) where ATP is produced aerobically is $P_a = \eta\eta_a Q_a^w$, whereas work power where ATP is produced by G is equal to $P_g = \eta\eta_g Q_g$. The work power where ATP is produced by CK is equal to $P_{ck} = \eta\eta_{ck} Q_{ck}$. Here, Q_a^w, Q_g and Q_{ck} represent the aerobic power, the power due to the G and the power due to the CK reaction (alactic power) respectively. These powers are different from the corresponding work powers due to heat production. Note that the aerobic power does not account for resting aerobic power (in our case estimated to be Q_r = 85 J/s). The total aerobic

power is $Q_a = Q_a^w + Q_r$. The two chemical-coupling efficiencies η_g and η_a are similar, whereas η_{ck} is larger [15]. Total work power $\tilde{P}$ is given by

$$\tilde{P} = P_a + P_{ck} + P_g = \eta\eta_a Q_a^w + \eta\eta_{ck} Q_{ck} + \eta\eta_g Q_g. \tag{1}$$

We propose that the $\tilde{P}$ associated with a specified work rate (P) is generally given as

$$\tilde{P} \overset{\text{mod}}{=} p_0 + c_P P, \tag{2}$$

where p_0 and c_P denote constants for our incline of 0.105, and '*mod*' means model assumption. During steady-state exercise below the LT, $Q_{ck} = Q_g = 0$, $\eta\eta_a = \bar{\eta}\bar{\eta}_a$, where the bars means the steady-state values in time of the efficiencies. We achieve from Equations (1) and (2) that

$$\tilde{P} = \bar{\eta}\bar{\eta}_a Q_a^w = p_0 + c_p P \Rightarrow Q_a^w = \frac{p_0 + c_p P}{\bar{\eta}\bar{\eta}_a} = q_0 + cP, q_0 = \frac{p_0}{\bar{\eta}\bar{\eta}_a}, c = \frac{c_p}{\bar{\eta}\bar{\eta}_a}. \tag{3}$$

For low exercise intensities, $\bar{\eta}\bar{\eta}_a$ may be assumed as constant for different intensities. Then q_0 and c denote constants for our chosen incline of 0.105. q_0 and c are simply established by applying a linear regression analysis on the measured aerobic power Q_a^w vs. the work rate P at low steady-state intensity. p_0 and c_P are then given by $p_0 = q_0\bar{\eta}\bar{\eta}_a$ and $c_p = c\,\bar{\eta}\bar{\eta}_a$. In this article, we set q_0 to 0 as an approximation, while c = 6.25 [13].

Model 1

At a sustained steady-state work rate, aerobic power reaches a steady state within 2 to 3 min [9]. To account for this delay, mathematically Stirling et al. [4] used a first-order differential equation. Our Model 1 is analogous to this differential equation model. The aerobic power due to the work rate ($Q_a^w(t) = Q_a(t) - Q_r$) is found by solving the following equation:

Model 1:

$$\dot{Q}_a^w(t) \overset{\text{mod}}{=} A Q_a^w(t)^B \left(Q_{\max} - Q_r - Q_a^w(t)\right)^C \left(\bar{Q}_{\text{vir}} - Q_a^w(t)\right)^E. \tag{4}$$

The 'dot' means time derivative, and $Q_{\max}$ denotes the maximum aerobic power. Here, we define the virtual aerobic power $\bar{Q}_{\text{vir}}$ for all intensities, also for use during non-steady-state situations [14].

$$\bar{Q}_{\text{vir}} = q_0 + cP. \tag{5}$$

Model 2

Our Model 2 is also a first-order differential equation model with the work rate as input as earlier forecasted [12,13].

Model 2:

$$\dot{Q}_{\text{vir}}(t) \overset{\text{mod}}{=} \frac{\bar{Q}_{\text{vir}} - Q_{\text{vir}}(t)}{\tau_a}, Q_a^w(t) = \text{Min}(Q_{\max} - Q_r - Q_{\text{vir}}(t)), \tag{6}$$

where τ_a is the time parameter characterizing the time at which aerobic power attains a steady-state asymptotically during constant work rate. The Min function ensures that the aerobic power $Q_a^w(t)$ is below $Q_{\max} - Q_r$. Reaching steady state means less than 1% change in aerobic power per second. Model 1 and Model 2 differ in the way they handle intensities above $Q_{\max}$. When B = 0, C = 0 and E = 1, Model 1 and Model 2 are alike given that, $A = 1/\tau_a$ and intensities are also below $Q_{\max}$. In this article, we propose that B = 0, C = 1 and E = 1 for Model 1 and A is fitted to the measurements.

Model 3

The contraction-coupling efficiency (η) or the aerobic chemical-coupling efficiency (η_a) may vary with time due to high exercise intensity. Reduced efficiency leads to a higher aerobic power for the same work rate, and this may explain the delayed superimposed slow aerobic component on the steady-state aerobic power. In order to account for this phenomenon, we set our third and new model

Model 3:

$$\dot{P}_{\text{vir}}(t) \overset{\text{mod}}{=} \frac{\tilde{P} - P_{\text{vir}}(t)}{\tau_a}, Q_a^w(t) = \text{Min}\big(Q_{\max} - Q_r, P_{\text{vir}}(t)/(\eta\eta_a)\big). \tag{7}$$

This equation describes the need for aerobic work power to fully accommodate the work rate.

For example, given that $\alpha = \eta\eta_a$ is a constant through time, we derive from Equation (7) that

$$\dot{P}_{\text{vir}}/(\eta\eta_a) = \frac{\big(\tilde{P}/(\eta\eta_a) - P_{\text{vir}}/(\eta\eta_a)\big)}{\tau_a} \Rightarrow \dot{Q}_{\text{vir}} = \frac{\left(\overbrace{\tilde{P}/(\eta\eta_a)}^{\bar{Q}_{\text{vir}}} - Q_{\text{vir}}\right)}{\tau_a} = \frac{\bar{Q}_{\text{vir}} - Q_{\text{vir}}}{\tau_a}. \tag{8}$$

Thus, Model 3 equals Model 2 only if $\eta\eta_a$ is constant for a specified time frame. If $\eta(t)\eta_a(t)$ decreases slowly with time, Equation (7) is the same, while $Q_a^w(t)$ increases slowly due to the $P_{\text{vir}}(t)/(\eta\eta_a)$. This gives a delayed superimposed aerobic power.

Model 4

As a forth model, we forecast the new model.

Model 4:

$$\dot{P}_{\text{vir}} \overset{\text{mod}}{=} \frac{\tilde{P} - P_{\text{vir}}(t)}{\tau_a} - \frac{P_g(t)}{\tau_a}, P_g(t) = \eta\eta_g Q_g, Q_a^w(t) = \text{Min}\big(Q_{\max} - Q_r, P_{\text{vir}}(t)/(\eta\eta_a)\big). \tag{9}$$

Although the model so far seems ad hoc, some interesting consequences can be deduced to support the model. Considering first constant efficiencies, we derive from Equation (9) after multiplying with $1/(\eta\eta_a)$

$$\begin{aligned} \dot{Q}_{\text{vir}}(t) &= \tfrac{\bar{Q}_{\text{vir}} - Q_{\text{vir}}(t)}{\tau_a} - \tfrac{\eta_g}{\eta_a\tau_a} Q_g(t) \\ Q_a^w &= \text{Min}(Q_{\max} - Q_r, Q_{\text{vir}}(t)). \end{aligned} \tag{10}$$

In order to further elucidate on Equation (10), we have from Equation (3) that $\tilde{P} = p_0 + c_p P = p_0 + (c_p/c)(\bar{Q}_{\text{vir}} - q_0)P = q_0\bar{\eta}\bar{\eta}_a + \bar{\eta}\bar{\eta}_a(\bar{Q}_{\text{vir}} - q_0)P = \bar{\eta}\bar{\eta}_a\bar{Q}_{\text{vir}}$, which may be seen as a generalized accumulated oxygen deficit model [13,16]. Thus we have

$$\eta\eta_a Q_a^w + \eta\eta_{ck} Q_{ck} + \eta\eta_g Q_g = \tilde{P} = \bar{\eta}\bar{\eta}_a\bar{Q}_{\text{vir}}. \tag{11}$$

Assuming that the exercise intensity is significantly below the LT, we set that $\eta\eta_a \approx \bar{\eta}\bar{\eta}_a$. Equation (11) can be reorganized algebraically and expressed as

$$Q_{ck} = \frac{\eta_a}{\eta_{ck}}\left(\bar{Q}_{\text{vir}} - Q_a^w - \frac{\eta_g}{\eta_a} Q_g\right). \tag{12}$$

Below the LT, we also have that $Q_{\text{vir}} = Q_a - Q_r = Q_a^w$. Applying Equations (10) and (12), we derive

$$Q_{ck} = \frac{\eta_a}{\eta_{ck}}\left(\bar{Q}_{\text{vir}} - Q_{\text{vir}} - \frac{\eta_g}{\eta_a}Q_g\right) = \frac{\eta_a\tau_a}{\eta_{ck}}\dot{Q}_a^w = \frac{\eta_a\tau_a}{\eta_{ck}}\dot{Q}_a. \tag{13}$$

Thus, we find that the alactic power Q_{ck} is proportional to the rate of change of the aerobic power [12]. Model 4 is thus consistent with the generalized oxygen accumulated oxygen deficit model, and we deduce that if the intensity is below the LT, the alactic power is proportional to the rate of change of the aerobic power.

The cardio-dynamic phase, which represents the circulatory transit delay from muscles to lungs, was not considered because the focus of the study was on actual aerobic power. Typical values of τ_a for moderate-intensity exercise range between 23 and 36 s [17–19]. di Prampero and Ferretti suggest 10–24 s [14]. Some studies have established that τ_a increases linearly with concentration of lactate [20], whereas others observed that τ_a = 23 s for all work rates [21]. The 2.83 m/s run (see our protocol described below) gives least scatter in the aerobic data for the transient period during increasing aerobic power. We therefore chose τ_a = 23 s and 1/A = 16,380 J based on the least root mean square (RMS) error between experimental data and the different models during the first 100 s at 2.83 m/s.

Contraction-coupling efficiency

The contraction-coupling efficiency is assumed to be $\eta \approx 0.5$ and chemical efficiency related to aerobic is $\eta_a = 0.3 - 0.7$. We use $\eta_a \approx 0.6$. With regard to alactic power, we forecast that η_{ck} is close to 1. We set η_{ck} = 0.95. With regard to lactic power, we set that $\eta_g \approx 0.3$. Amount of heat generated per used ATP is found to be about two times larger in oxidative phosphorylation and anaerobic glycolysis compared to ATP from CK [15]. The number of ATP generated per used oxygen is theoretically estimated to be about 6. However, studies reveal that when exercise intensity is equal to or above LT, ATP utilization increases and contraction-coupling efficiency decreases for a constant work rate. This may in part be explained by a change in fibre-type recruitment, an elevated temperature, lowered pH or increased Pi levels [19]. Thus, a lower contraction-coupling efficiency of muscle contractions and a lower P/O ratio could simply explain lack of steady-state ATP consumption for a given work rate. We forecast that efficiencies during production and use of ATP may dependent mainly on the pH and thereby strongly correlate to the lactate concentration. To account for a model with time-varying parameters, we set that $\eta\eta_a$ and $\eta\eta_g$ depend on the lactate concentration. As a model, we set that $\eta\eta_a(t) = \eta_0\eta_{0a}\Omega(C(t))$ and $\eta\eta_g(t) = \eta_0\eta_{0g}\Omega(C(t))$ where $\Omega(C(0)) = 1$, $\eta_0 = 0.5$, $\eta_{0a} = 0.6$, $\eta_{0g} = 0.3$. The Ω function describes reduction in efficiencies due to lactate concentration C (Figure 1). We apply the hypothetical inductive–deductive method. Thus, the simulated consequences (deductions) of this assumption (Figure 1) are what we compare with the experiments. The data are not extensive enough to uniquely construct how efficiencies reduce with increasing lactate concentration. Thus, as a simplified model, we let the efficiencies decrease linearly with increasing lactate concentration. The decline we establish by inverse modelling.

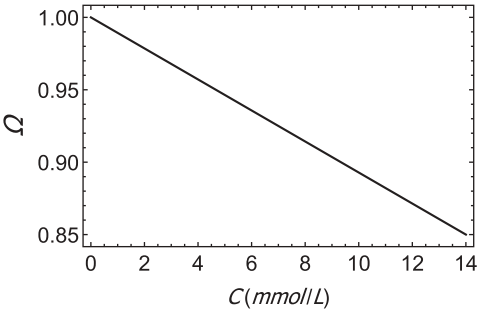

Figure 1. A postulated scaled efficiency $\Omega(C)$ as a function of the lactate concentration C in mmol/L.

Lactic power

The model in Equation (9) requires lactic power as input. In this study, we used changes in blood lactate concentration measured in mmol/L to indicate changes in lactic power. Here, the change in lactate was converted into lactic power following the relationship indicated by di Prampero and Ferretti [14]. Using that formula, 1 mmol/L blood lactate corresponds to 2.7–3.3 mL/kg O_2. We set that 1 mL of O_2 is 20 J. Lactic power in J/s is set to $2.7 \times 20\, m\, \dot{C}$, where $\dot{C}$ is the rate of change in blood lactate concentration in mmol/L blood, and m is the mass of the skier. It is worth noticing that there are several shortcomings of using this formula, for example that blood lactate concentration can differ significantly from muscle lactate concentration in dynamic situations, that lactate produced is oxidized in several body tissues and that the concentration in the blood is additionally influenced by blood volume and the type of exercise. This gives an error margin in the analysis. However, the formula has repeatedly showed valid results, so we regard it as our best tool in our case.

Experimental test

The characteristics of the skier were as following: body mass of m = 78 kg, body height of 181 cm, VO_2max (Q_{max}) = 1870 J/s and LT power Q_{LT}= 1650 J/s.

All treadmill tests were performed on a 6 × 3 m motor-driven treadmill (Bonte Technology, Zwolle, The Netherlands). Inclination and speed were calibrated using the Qualisys Pro Reflex system and the Qualisys Track Manager software (Qualisys AB, Gothenburg, Sweden). The treadmill belt consisted of a non-slip rubber surface that allowed the skier to use his own poles (pole length: 80% of body height) with special carbide tips.

An open-circuit indirect calorimetry (Oxycon Pro apparatus with a mixing chamber) was used to measure gas exchange values (Jaeger GmbH, Hoechberg, Germany). Before each measurement, the VO_2 and VCO_2 gas analysers were calibrated using high-precision gases (16.00 ± 0.04% O2 and 5.00 ± 0.1% CO_2, Riessner-Gase GmbH & co, Lichtenfels, Germany). The inspiratory flowmeter was calibrated with a 3-L volume syringe (Hans Rudolph Inc., Kansas City, MO, USA). Blood lactate concentration (BLa) was measured on 5 µL samples taken from the fingertip by a Lactate Pro LT-1710 t (ArkRay Inc., Kyoto, Japan).

The experimental protocols followed the order described below. Training on the days before testing was standardized, and the subject drank a standard fluid with sugar and electrolytes during all breaks while testing. Before each testing session, a standardized 20-min warm-up was performed. All tests were performed at constant work rates with 0.105 radians inclinations. On four separate days, the skier ran at 2.33, 2.83, 3.08 and 3.19 m/s, respectively. The first three speeds were below LT, whereas the highest was slightly above (but below Q_{max}). On a fifth day to the skier ran for at 3.88 m/s, which is about 9% above Q_{max}. Following all tests, a subsequent recovery period followed the exercise. VO_2 was continuously measured, and blood lactate concentration taken at different time points throughout all exercise and recovery. See figures in the results for more details about the various protocols.

VO_2max was tested at an inclination of 0.105 radians, with an initial speed of 3 m/s followed by 0.3 m/s increase in speed every minute until exhaustion. VO_2 was measured continuously and the average of the three highest 10-s consecutive measurements determined VO_2max and used for calculations of maximal aerobic metabolic power. The test was considered to be at maximal effort based on three criteria: (1) a plateau in VO_2 is obtained with increasing exercise intensity, (2) respiratory exchange ratio is above 1.10 and (3) blood lactate concentration exceeds 8 mmol/L.

We summarize the parameters that are used in Table 1.

Results

Figure 2 shows the simulated and experimental results for the lowest exercise intensity (0.66 Q_{max}). A visual inspection shows that all models fit reasonably well with the experimental data,

Table 1. The parameters used in the models.

Q_{max}	Q_r	c	m	$\eta_0\eta_{0a}$	$\eta_0\eta_{0g}$	Ω	τ	1/A
1870 J/s	85 J/s	6.25	78 kg	0.3	0.15	Figure 1	23 s	*16,380 Js*

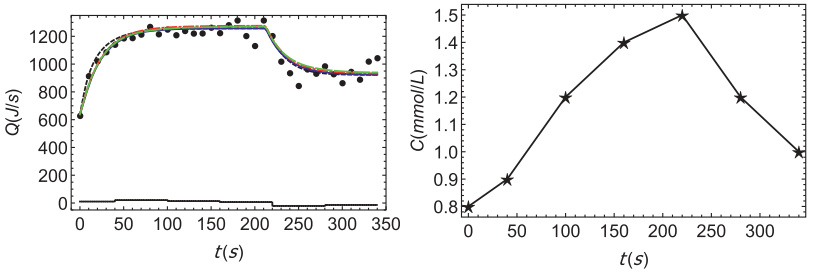

Figure 2. (a) The powers Q in J/s as a function of time (*t*) for an elite skier while running with poles on a treadmill at an incline of 0.105 and speed of 8.4 km/h = 2.33 m/s. (b) The lactate concentration as a function of time for an elite skier while running with poles on a treadmill at an incline of 0.105 and speed of 8.4 km/h = 2.33 m/s.

_ _ _ _ _: *Simulated aerobic power using Model 1*
_____: *Simulated aerobic power using Model 2*
__ _ __ _: *Simulated aerobic power using Model 3*
___ ___: *Simulated aerobic power using Model 4*
. . . .: *Simulated anaerobic lactic power*
●: *Aerobic power measured in the experiment*

although the simulated steady-state value is too high. For some reason, the measured VO_2 scatters more during the recovery period.

Figure 3 shows VO_2 at an intensity below the LT (0.80 Q_{max}). Here, Models 1 and 2 fit reasonably well to the data, but they do not account for the delayed superimposed aerobic power. Models 3 and 4 fit this better and give higher aerobic power due to the delayed superimposed aerobic power, which is caused by the lower efficiencies utilized (see Figure 1). An indication of delayed VO_2 kinetic (after accounting for lactic power) is observed for Model 4, which consequently provides better fit better than Model 3 during the recovery period.

Figure 4 illustrates that an intensity close to the LT (0.87 Q_{max}) reveals a non-steady delayed superimposed aerobic power which Models 1 and 2 fail to account for. The delayed slow superimposed component of aerobic power in Model 3 appears to be too large, whereas Model 4 provides the best fit to the data.

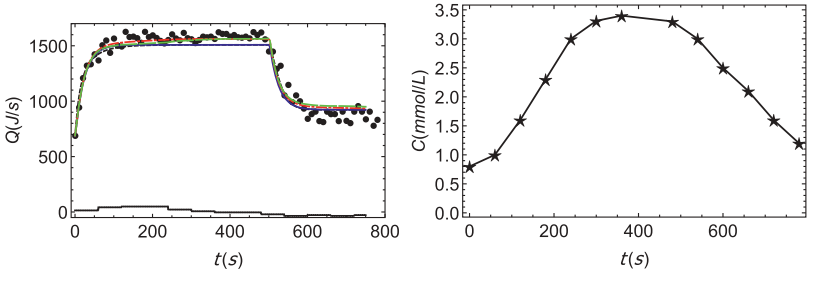

Figure 3. (a) The powers Q in J/s as a function of time (*t*) for an elite skier while running with poles on a treadmill at an incline of 0.105 and speed of 10.2 km/h = 2.83 m/s. (b) The lactate concentration as a function of time for an elite skier while running with poles on a treadmill at an incline of 0.105 and speed of 10.2 km/h = 2.83 m/s.

_ _ _ _ _: *Simulated aerobic power using Model 1*
_____: *Simulated aerobic power using Model 2*
__ _ __ _: *Simulated aerobic power using Model 3*
___ ___: *Simulated aerobic power using Model 4*
. . . .: *Simulated anaerobic lactic power*
●: *Aerobic power measured in the experiment*

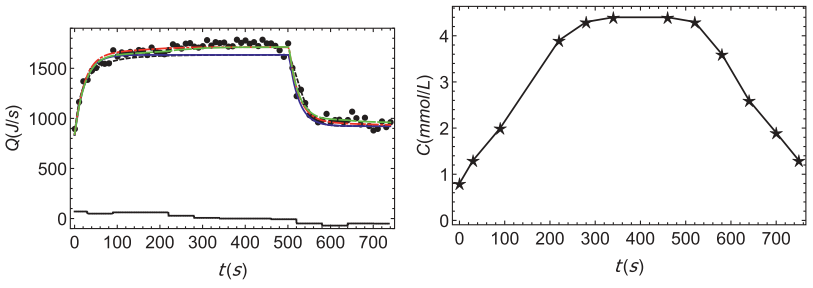

Figure 4. (a) The powers Q in J/s as a function of time (*t*) for an elite skier while running with poles on a treadmill at an incline of 0.105 and speed of 11.1 km/h = 3.08 m/s. (b) The lactate concentration as a function of time for an elite skier while running with poles on a treadmill at an incline of 0.105 and speed of 11.1 km/h = 3.08 m/s.

_ _ _ _ _: *Simulated aerobic power using Model 1*
_____: *Simulated aerobic power using Model 2*
__ _ __ _: *Simulated aerobic power using Model 3*
___ ___: *Simulated aerobic power using Model 4*
. . ..: *Simulated anaerobic lactic power*
●: *Aerobic power using from experimental data*

In Figure 5, the intensity is above LT (0.90 Q_{max}) in which Models 3 and 4 show a superimposed delayed slow component, while Models 1 and 2 did not fit well. Model 4 seems to provide the best fit to the data although it is notable that Model 3 fits somewhat better than Model 4 during the recovery period.

Figure 6 shows an intensity above VO_2max (1.09 Q_{max}). Here, Model 1 shows too slow VO_2 kinetics, while Models 2 and 3 show too fast VO_2 kinetics. Models 3 and 4 reach maximal aerobic power after 50 and 60 s, respectively, and the delayed superimposed slow component of aerobic power is better predicted. However, discrepancies are seen during the recovery period for all models. Table 2 shows an RMS error between model and data.

At intensities below 70% of LT, the lactate concentration is lower than 1.5 mmol/L and the slow component of the VO_2 is negligible. Between 70% of LT and LT, the lactate concentration is between 1.5 and 4.5 mmol/L. The slow component of VO_2 is significant and VO_2 drifts starts from 100 to 200 s and reaches a steady state of VO_2 that is lower than VO_2max. At intensities between LT and VO_2max, the slow component interferes directly with the VO_2 kinetics and generates a VO_2 that approaches VO_2max. Finally, at intensities above VO_2max, the VO_2 reaches VO_2max relatively early and the slow component is of less importance. The exercise is terminated by the athlete after some time (approximately 150 s). We have also made a table related to this (Table 3).

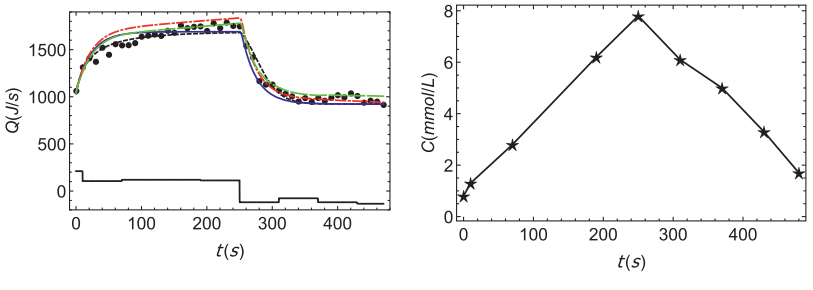

Figure 5. (a) The powers Q in J/s as a function of time (*t*) for an elite skier while running with poles on a treadmill at an incline of 0.105 and speed of 11.5 km/h = 3.19 m/s. (b) The lactate concentration as a function of time for an elite skier while running with poles on a treadmill at an incline of 0.105 and speed of 11.5 km/h = 3.19 m/s.

_ _ _ _ _: *Simulated aerobic power using Model 1*
_____: *Simulated aerobic power using Model 2*
__ _ __ _: *Simulated aerobic power using Model 3*
___ ___: *Simulated aerobic power using Model 4*
. . ..: *Simulated anaerobic lactic power*
●: *Aerobic power measured in the experiment*

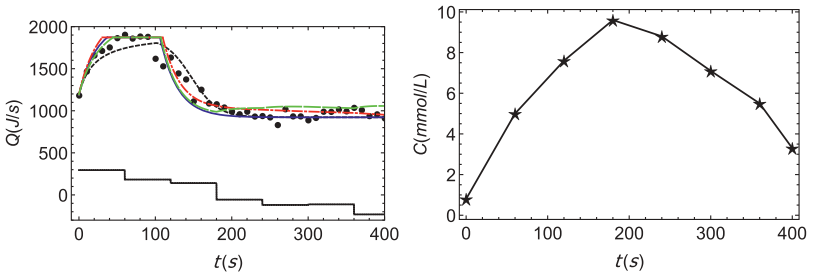

Figure 6. (a) The powers Q in J/s as a function of time (*t*) for an elite skier while running with poles on a treadmill at an incline of 0.105 and speed of 14.0 km/h = 3.88 m/s. (b) The lactate concentration as a function of time for an elite skier while running with poles on a treadmill at an incline of 0.105 and speed of 14.0 km/h = 3.88 m/s.

_ _ _ _ _: *Simulated aerobic power using Model 1*
_____: *Simulated aerobic power using Model 2*
__ _ __ _: *Simulated aerobic power using Model 3*
___ ___: *Simulated aerobic power using Model 4*
. . ..: *Simulated anaerobic lactic power*
●: *Aerobic power measured in the experiment*

Table 2. The root mean square error between the models and the data.

	Model 1	Model 2	Model 3	Model 4
V = 8.4 km/h	53.45	54.72	58.43	57.89
V = 10.2 km/h	75.75	78.13	62.37	69.13
V = 11.1 km/h	84.59	82.04	46.85	45.08
V = 11.5 km/h	64.97	73.38	80.60	57.16
V = 14.0 km/h	96.72	102.74	92.24	109.53

Table 3. Aspects related to oxygen uptake kinetics during exercise at different intensities.

Intensity < 70%	70% < Intensity <LT	LT < Intensity < VO_2max	VO_2max < Intensity
Lactate level is steady and less than 1.5	Lactate level is steady state between 1.5 and 4.5	No steady-state level of lactate	VO_2 reaches VO_2max relatively early and the slow component is of less importance
No significant slow component of VO_2	Significant slow component of VO_2 Steady-state VO_2 is somewhat lower than VO_2max	Slow component of VO_2 interferes with VO_2 kinetics and generates a VO_2 that approaches VO_2max	Exercise is terminated by the athlete after some time

Conclusions

In this study, we elucidated four different mathematical models for the kinetics of oxygen uptake during whole-body exercise at different intensities and throughout the subsequent recovery periods. We employ the hypothetical inductive–deductive method and study four different models for the VO_2 kinetics, in which two of them have not previously been presented in the literature. The VO_2 development using these models compared with experimental results where an elite cross-country skier performed laboratory tests while running with poles on a treadmill. The most developed model accounted for the delayed superimposed slow component of VO_2 and the influence of lactic power production on VO_2 kinetics. The rate of change of VO_2 of this model is consistent with the accumulated oxygen deficit model and matched the data well, even for intensities above the LT and during recovery.

The three other models were also able to predict VO_2 kinetics fairly well. Our Model 1, that is a modified version of Stirling et al.'s [4] differential equation, shows good agreement at low intensity and during the recovery periods, but fails to account for the superimposed slow component when exercising at high intensities. The same applies to Model 2 where the time

development of VO_2 associated with a given work rate [12,13] does not account for the superimposed slow component.

This was improved in Model 3 where the chemical- and contraction-coupling efficiencies associated with production of high lactic power during high exercise intensity was accounted for. This model induces a superimposed delayed slow component of VO_2 that fits the data better than Models 1 and 2 at high intensities and indicate that reduced chemical- and contraction-coupling efficiencies are present at high intensities where high lactic power is produced. Specifically, we modelled that efficiencies decrease as a function of lactate concentration to account for the delayed superimposed slow component of aerobic power. We do not propose that the increased blood lactate concentrations directly influence these efficiencies. However, it is likely that the coinciding reduction in muscle pH does. Although this seems to have improved Model 3 at high intensity, it gives somewhat too high aerobic power during steady state. Model 3 shows 40% higher RMS than model 4 at 11.5 km/h (3.19 m/s), while Model 4 only shows 19% higher RMS than Model 3 at 14.0 km/h (3.88 m/s). Therefore, in Model 4, we further assume that also the aerobic kinetics is influenced by lactic power production, which altogether may capture the data best.

Cross-country skiing is performed at varying exercise intensities, with the uphill parts performed at high intensity well above what can be done aerobically, whereas downhill terrain allows for recovery. This shows an importance of understanding the factors influencing oxygen kinetics above aerobic steady-state exercise and during recovery. Uniquely for this study, our most developed model could account for the delayed superimposed slow component of oxygen uptake and the influence of lactic power production on the oxygen kinetics.

Although we consider the elite skier to be a representative subject, other skiers would have different characteristics and generate slightly different aggregated data and behaviour. In this study, we did not perform any repeated measures of performance of our skier, which might be regarded a weakness of the current design. However, results from national and international competitions, as well as performance tests in our laboratory, indicate that elite skiers are able to reproduce performance by a standard deviation of less than 2%.

Disclosure statement

No potential conflict of interest was reported by the authors.

Authors' contributions

JFM performed the mathematical simulations while ØS performed the laboratory testing. Both authors contributed with important intellectual content in all parts of the manuscript. Both authors read and approved the final manuscript.

References

[1] O. Sandbakk, G. Ettema, S. Leirdal, V. Jakobsen, and H.C. Holmberg, *Analysis of a sprint ski race and associated laboratory determinants of world-class performance*, Eur. J. Appl. Physiol. 111 (2011), pp. 947–957. doi:10.1007/s00421-010-1719-9

[2] O. Sandbakk and H.C. Holmberg, *A reappraisal of success factors for Olympic cross-country skiing*, Int. J. Sports Physiol. Perform. 9 (2014), pp. 117–121. doi:10.1123/ijspp.2013-0373

[3] T.J. Barstow, N. Lamarra, and B.J. Whipp, *Modulation of muscle and pulmonary O2 uptakes by circulatory dynamics during exercise*, J. Appl. Physiol. 68 (1990), pp. 979–989.

[4] J. Stirling, M. Zakynthinaki, and B. Saltin, *A model of oxygen uptake kinetics in response to exercise: Including a means of calculating oxygen demand/deficit/debt*, Bull. Math. Biol. 67 (2005), pp. 989–1015. doi:10.1016/j.bulm.2004.12.005

[5] J.M. Murias, M.D. Spencer, J.M. Kowalchuk, and D.H. Paterson, *Influence of phase I duration on phase II VO2 kinetics parameter estimates in older and young adults*, Am. J. Physiology-Regulatory, Integr. Comp. Physiol. 301 (2011), pp. R218–R224. doi:10.1152/ajpregu.00060.2011

[6] V. Billat, B. Bocquet, J. Slawinski, and L. Laffite, *Effects of a prior intermittent run at vVO2MAX on oxygen kinetics during an all-out severe run in humans*, J. Sports Med. Phys. Fitness 40 (2000), pp. 185.
[7] B. Grassi, H.B. Rossiter, and J.A. Zoladz, *Skeletal muscle fatigue and decreased efficiency: Two sides of the same coin?* Exerc Sport Sci Rev 43 (2015), pp. 75–83. doi:10.1249/JES.0000000000000043
[8] A.M. Jones, B. Grassi, P.M. Christensen, P. Krustrup, J. Bangsbo, and D.C. Poole, *Slow component of VO2 kinetics: Mechanistic bases and practical applications*, Med. Sci. Sports Exerc. 43 (2011), pp. 2046–2062. doi:10.1249/MSS.0b013e31821fcfc1
[9] H.B. Rossiter, *Exercise: Kinetic considerations for gas exchange*, Compr. Physiol. 1 (2011), pp. 203–244.
[10] T.J. Barstow, *Characterization of VO2 kinetics during heavy exercise*, Med. Sci. Sports. Exerc. 26 (1994), pp. 1327–1334. doi:10.1249/00005768-199411000-00006
[11] G.A. Gaesser and D.C. Poole, *The slow component of oxygen uptake kinetics in humans*, Exerc. Sport Sci. Rev. 24 (1996), pp. 35–70. doi:10.1249/00003677-199600240-00004
[12] J.F. Moxnes and Ø. Sandbakk, *The kinetics of lactate production and removal during whole-body exercise*, Theor. Biol. Med. Model. 9(2012). doi:10.1186/1742-4682-9-7
[13] J.F. Moxnes, K. Hausken, and Ø. Sandbakk, *On the kinetics of anaerobic power*, Theor. Biol. Med. Modelling 9 (2012), pp. 29. doi:10.1186/1742-4682-9-29
[14] P.E. di Prampero and G. Ferretti, *The energetics of anaerobic muscle metabolism: A reappraisal of older and recent concepts*, Respir. Physiol. 118 (1999), pp. 103–115. doi:10.1016/S0034-5687(99)00083-3
[15] J. González-Alonso, B. Quistorff, P. Krustrup, J. Bangsbo, and B. Saltin, *Heat production in human skeletal muscle at the onset of intense dynamic exercise*, J. Physiol. 524 (2000), pp. 603–615. doi:10.1111/j.1469-7793.2000.00603.x
[16] J.I. Medbo, A.-C. Mohn, I. Tabata, R. Bahr, O. Vaage, and O.M. Sejersted, *Anaerobic capacity determined by maximal accumulated O2 deficit*, J. Appl. Physiol. 64 (1988), pp. 50–60.
[17] P.E. di Prampero, *Factors limiting maximal performance in humans*, Eur. J. Appl. Physiol. 90 (2003), pp. 420–429. doi:10.1007/s00421-003-0926-z
[18] T. Losnegard, H. Myklebust, and J. Hallén, *Energy System Contribution as a Determinant of Performance in Elite Skiers*, Med. Sci. Sports Exerc. 2011. ISSN: 1530-0315.
[19] J. Bangsbo, P. Krustrup, J. González-Alonso, and B. Saltin, *ATP production and efficiency of human skeletal muscle during intense exercise: Effect of previous exercise*, Am. J. Physiol. Endocrinol. Metab. 280 (2001), pp. E956–E964.
[20] P. Cerretelli, D. Pendergast, W. Paganelli, and D. Rennie, *Effects of specific muscle training on VO2 on-response and early blood lactate*, J. Appl. Physiol. 47 (1979), pp. 761–769.
[21] T. Binzoni, G. Ferretti, K. Schenker, and P. Cerretelli, *Phosphocreatine hydrolysis by 31P-NMR at the onset of constant-load exercise in humans*, J. Appl. Physiol. 73 (1992), pp. 1644–1649.